

Heterogeneous Reactions of ClONO₂, HCl, and HOCl on Liquid Sulfuric Acid Surfaces

Renyi Zhang,* Ming-Taun Leu,* and Leon F. Keyser

Earth and Space Sciences Division, Jet Propulsion Laboratory, California Institute of Technology, Pasadena, California 91109

Received: August 24, 1994; In Final Form: October 12, 1994[⊗]

The heterogeneous reactions of ClONO₂ + H₂O → HNO₃ + HOCl (1), ClONO₂ + HCl → Cl₂ + HNO₃ (2), and HOCl + HCl → Cl₂ + H₂O (3) on liquid sulfuric acid surfaces have been studied using a fast flow reactor coupled to a quadrupole mass spectrometer. The main objectives of the study are to investigate (a) the temperature dependence of these reactions at a fixed H₂O partial pressure typical of the lower stratosphere (that is, by changing temperature at a constant water partial pressure, the H₂SO₄ content of the surfaces is also changed), (b) the relative importance or competition between reactions 1 and 2, and (c) the effect of HNO₃ on the reaction probabilities due to the formation of a H₂SO₄/HNO₃/H₂O ternary system. The measurements show that all the reactions depend markedly on temperature at a fixed H₂O partial pressure: they proceed efficiently at temperatures near 200 K and much slower at temperatures near 220 K. The reaction probability (γ₁) for ClONO₂ hydrolysis approaches 0.01 at temperatures below 200 K, whereas the values for γ₂ and γ₃ are on the order of a few tenths at 200 K. Although detailed mechanisms for these reactions are still unknown, the present data indicate that the competition between ClONO₂ hydrolysis and ClONO₂ reaction with HCl may depend on temperature (or H₂SO₄ wt %): in the presence of gaseous HCl at stratospheric concentrations, reaction 2 is dominant at lower temperatures (<200 K), but reaction 1 becomes important at temperatures above 210 K. Furthermore, reaction probability measurements performed on the H₂SO₄/HNO₃/H₂O ternary solutions do not exhibit noticeable deviation from those performed on the H₂SO₄/H₂O binary system, suggesting little effect of HNO₃ in sulfate aerosols on the ClONO₂ and HOCl reactions with HCl. The results reveal that significant reductions in the chlorine-containing reservoir species (such as ClONO₂ and HCl) can take place on stratospheric sulfate aerosols at high latitudes in winter and early spring, even at temperatures too warm for polar stratospheric clouds (PSCs) to form or in regions where nucleation of PSCs is sparse. This is particularly true under elevated sulfuric acid loading, such as that after the eruption of Mt. Pinatubo. Comparisons between our results and those presently available have also been made.

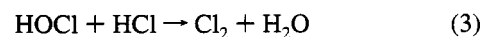
Introduction

It is now well established that heterogeneous reactions occurring on the surfaces of polar stratospheric cloud particles play a central role in the ozone depletion.¹ The surface-catalyzed reactions convert chlorine-containing reservoir species into photochemically reactive forms, leading to high rates of ozone destruction by active chlorine species, Cl and ClO. Of equal importance to the polar stratospheric ozone depletion is the concomitant removal of nitrogen oxides from the gas phase, which inhibits the formation of chlorine nitrate and subsequently leads to large concentrations of ClO. Such heterogeneous processing of reservoir chlorine species on PSC particles has been clearly seen in recent field observations, showing chemical changes such as the increase in ClO and concurrent decreases in HCl, ClONO₂, and ozone, as measured from inside to outside of the chemically perturbed regions in Antarctica and the Arctic.^{2–5} Furthermore, laboratory studies have documented that these heterogeneous reactions proceed efficiently on the PSC materials,⁶ which are believed to consist of either nitric acid hydrates (type I) or ice (type II).^{7,8}

Similar reactions occurring on stratospheric sulfate aerosols have also been proposed to have a significant effect on the chemistry of the global stratosphere.^{9–11} The sulfate aerosol layer, which exists at altitudes between 10 and 30 km, is composed of aqueous sulfuric acid particles with a mean

diameter of about 0.1 μm and concentrations from 1 to 10 cm⁻³ under unperturbed stratospheric conditions. Major volcanic eruptions, such as the eruption of Mt. Pinatubo, may significantly increase the particle size and concentration. Steele et al.¹² first compiled the sulfate aerosol compositions as a function of temperature, predicting an aerosol concentration of 70–80 wt % at mid latitudes and of less than 50 wt % at high latitudes. Recent studies^{13–16} have suggested that, at lower temperatures such as those prevailing in the early polar winter, the sulfate aerosols absorb a significant amount of HNO₃, leading to the formation of a H₂SO₄/HNO₃/H₂O ternary system prior to the onset of PSCs. Additionally, on the basis of laboratory observations, crystalline sulfuric acid hydrates such as tetrahydrate and hemihexahydrate^{17,18} or monohydrate¹⁹ have been proposed to form and persist in certain stratospheric regions.

The heterogeneous reactions, which could promote chlorine activation and affect the stratospheric NO_x budget, are as follows:



On crystalline sulfuric acid tetrahydrate, reactions 1–3 have been shown to proceed efficiently at low temperatures (<200 K).^{24,25} Earlier solubility studies²⁶ reported a negligible amount

* To whom correspondence should be addressed.

⊗ Abstract published in *Advance ACS Abstracts*, November 15, 1994.

of HCl in liquid sulfate aerosols, too small for reactions 2 and 3 to occur at significant rates on the global stratosphere. In addition, other laboratory studies yielded very small uptake coefficients for these reactions on liquid sulfuric acid solutions.^{22,27} It is now clear that the rates of these two reactions are critically determined by the amount of HCl dissolved in the liquid solutions, which, in turn, depends on both temperature and aerosol acid content. Thus, changes in stratospheric temperatures (which will also change the sulfate aerosol concentration) would likely result in highly nonlinear behavior for these two reactions. Recent laboratory results predict an equilibrium HCl concentration as high as 0.1% by weight in the stratospheric sulfate aerosols at temperatures below 192 K and at an HCl mixing ratio of a few ppbv,¹⁵ an amount which would be consistent with reaction probabilities on the order of a few tenths for reactions 2 and 3.¹³ More recently, efforts have been made to calculate reaction probabilities based on laboratory measured quantities;^{28,29} a theoretical framework has been proposed to apply the laboratory data to the stratosphere. Chemical processing of air by stratospheric sulfate aerosols via reactions 2 and 3 at high latitudes is supported by recent AASE II observations,¹⁴ which reveal a significant depletion in both ClONO₂ and HCl column abundances in the Pinatubo plume, even when there is no PSC signature.

Another important heterogeneous reaction on liquid sulfate aerosols is



This reaction is believed to reduce the stratospheric NO_x concentration and consequently result in increases in the abundances of ClO and OH. Several laboratory results have concluded that the reaction probability for reaction 4 is independent of temperature, sulfuric acid concentration, and even particle size, with a value of about 0.1.^{20–23} There is now accumulating evidence that the observed abundance of nitrogen and chlorine species in mid latitudes cannot be simulated accurately in numerical models by gas phase processes alone, but that inclusion of N₂O₅ hydrolysis produces better agreement between observations and calculations. Conversely, the proposed formation of solid sulfuric acid particles in the stratosphere could potentially suppress the N₂O₅ hydrolysis and thus terminate this reaction channel.^{19,24}

The aim of this work is to perform direct laboratory experiments on liquid sulfuric acid surfaces under stratospheric conditions. The reaction probabilities for ClONO₂ hydrolysis and HCl reactions with ClONO₂ and HOCl at the reactant concentrations characteristic of the lower stratosphere have been measured. The temperature dependence of these reactions was investigated at a fixed H₂O partial pressure corresponding to a mixing ratio of about 5 ppmv at 100 mb (~16 km) and at temperatures from 195 to 220 K. The relative importance or competition between the hydrolysis of ClONO₂ and the ClONO₂ reaction with HCl was also examined so that accurate chlorine activation processes on the stratospheric sulfate aerosols can be applied and simulated in atmospheric models. Finally, we investigated the effect of HNO₃ on the reaction probabilities due to the formation of the ternary H₂SO₄/HNO₃/H₂O system, which has been proposed to occur prior to the onset of type I PSCs.

Experimental Approach

Reaction probability measurements were performed in a fast flow reactor attached to a differentially pumped quadrupole mass spectrometer. The reactor section is shown schematically in

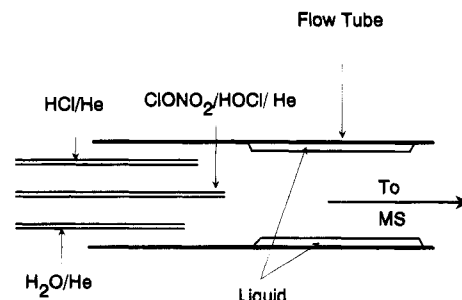


Figure 1. Schematic diagram of the flow reactor.

Figure 1. An overview of the experimental procedure is given here, and details of the apparatus have been discussed elsewhere.³⁰

The flow reactor, of inner diameter 2.8 cm and length 34.0 cm, was horizontally mounted and had three movable injectors located at the upstream end. A jacketed injector (1.0-cm o.d.) kept warm by circulating a room temperature solution of ethylene glycol in water was used to add H₂O and HNO₃ to the system. Normally, this injector was positioned near the upstream end to prevent possible warming of the substrate. The reactants (such as ClONO₂ or HOCl) were introduced through a centrally located unjacketed injector (0.3-cm o.d.), and a third unjacketed injector of similar o.d. was used to introduce HCl. All the gaseous species were delivered to the flow tube along with small He flow (0.1–5.0 cm³ min⁻¹ at STP) and further diluted in the main He flow (280 cm³ min⁻¹ at STP) before contacting the liquid surface. Typically, the flow reactor was operated at 0.5 Torr total pressure and 890 cm/s flow velocity.

Liquid H₂SO₄ films were prepared by totally covering the inside walls of the flow tube with sulfuric acid solutions. To ensure a uniform wetting, the flow tube was first cleaned with a dilute HF solution and then rinsed with distilled water. At low temperatures (<220 K) the solutions were sufficiently viscous to produce an essentially static film which lasted over the time scale of the experiments. The thickness of the liquid was estimated to be ~0.1 mm.

The sulfuric acid content initially used was less than 70 wt % to avoid possible freezing of the film at temperatures above 220 K. During the course of the experiments, the acid content can be varied by addition of H₂O through the jacketed injector; once exposed to H₂O, the sulfuric acid film took up H₂O and became more dilute until equilibrium was reached. Alternatively, compositional changes of the film can be made through evaporation of H₂O, by raising the flow tube temperature and by flowing dry helium over the sample. Critical parameters for the measurements were temperature and H₂O partial pressure, which determined the H₂SO₄ content (the temperature and H₂O partial pressure in the flow tube were used to estimate the acid content from the vapor pressure data of Zeleznik³¹ and Zhang et al.¹⁸). The error limit in estimating the H₂SO₄ content of the films was about 1–2 wt %, considering uncertainties associated with temperature (±1 K) and water partial pressure (±10%). For most experiments reported here, the H₂O partial pressure was closely maintained at 3.8 × 10⁻⁴ Torr (corresponding to 5 ppmv H₂O mixing ratio at 100 mb in the stratosphere) while the temperature was regulated from 195 to 220 K. This was equivalent to changing H₂SO₄ content from 45 to 70 wt %. Thus, by using H₂O partial pressures similar to those found in the stratosphere, the liquid film had compositions representative of stratospheric sulfate aerosols. Frequently, the film crystallized upon further cooling below 195 K.

For measurements of reactive uptakes of ClONO₂ and HOCl on sulfuric acid due to the reactions with HCl, the acid film

was first exposed to HCl vapor before introducing the reactant. In these measurements, it was important to ensure the equilibrium of HCl between the gas and liquid. This can be verified by pulling the HCl injector upstream while monitoring the HCl signal recovery in the mass spectrometer. Also, the gaseous HCl concentration had to be effectively maintained to offset changes in temperature or in H₂SO₄ content induced by addition or evaporation of H₂O. Similarly, HNO₃ was also introduced from the gas phase and allowed to equilibrate with the liquid.

Reaction probabilities (γ 's) were calculated from first-order rate constants obtained from the reactant loss or product growth. The surface area of sulfuric acid films was assumed to be the geometric area of the flow tube. Standard cylindrical flow tube analysis techniques were used.³² Corrections for gas phase diffusion were made by using the method developed by Brown.³³ The diffusion coefficients of ClONO₂, HOCl, and HCl were estimated using the method described by Marrero and Mason:³⁴ the values were 176, 215, and 296 Torr cm² s⁻¹ for ClONO₂, HOCl, and HCl at 200 K, respectively. A temperature dependence of $T^{1.75}$ was employed. The Brown correction was approximately 10% for small γ values ($\gamma < 0.01$) and as large as a factor of 4 for large values ($\gamma > 0.2$).

ClONO₂ was synthesized by the reaction of Cl₂O with N₂O₅³⁵ and was eluted from a trap at 192 K through a metering valve with a He flow of 0.1–5.0 cm³ min⁻¹ at STP. In calibrating ClONO₂, He was flowed through the ClONO₂ sample kept at 144 K, and the ClONO₂ concentration in the flow tube was estimated by assuming full saturation of the He flow when it exited the ClONO₂ trap. HOCl was produced by passing ClONO₂ through a 40 wt % H₂SO₄ solution at 273 K. This source was stable during the experiment and contained few impurities. The HOCl concentration was estimated by its production from reaction 1 on a liquid H₂SO₄ film. For this case, a stoichiometric ratio of unity was assumed for HOCl formed due to ClONO₂ lost (justification is given below). HCl was added to the flow tube from a dilute mixture in He (0.1–5.0%), and its concentration was determined either by observing the pressure rise in the flow tube upon its addition or by using a 10 cm³ min⁻¹ (at STP) mass flow meter. HNO₃ was collected from a 3:1 solution of H₂SO₄ (96 wt %) and HNO₃ (70 wt %) and was calibrated similarly to HCl. Water signals were calibrated by depositing an ice film and using its vapor pressure over the temperature range of 190–230 K.³⁶

HCl, HOCl, and Cl₂ were monitored at their parent peaks of 36, 52, and 70, respectively. ClONO₂ and HNO₃ were both detected at $m/e = 46$, which corresponds to the NO₂⁺ ion fragment. Detection limits were about 5×10^{-8} Torr for ClONO₂, Cl₂, HOCl, and HNO₃ and 1×10^{-7} Torr for HCl. These detection sensitivities were limited mainly by background partial pressures. During the experiments, all the relevant mass spectrometer signals were simultaneously recorded by using a computer data acquisition system.

Results

Observations of Physical Uptake of HCl, HOCl, and HNO₃ on Liquid Sulfuric Acid. Because HCl and HNO₃ were added to the liquid sulfuric acid films by allowing the acid surface to equilibrate with the vapors introduced with the carrier gas, it was essential to understand their adsorption behavior on H₂SO₄ over the temperature and acid content range investigated. Also, HOCl formed by the reaction of ClONO₂ with H₂O may be retained in the H₂SO₄ solution, possibly affecting the γ values determined. Furthermore, for the HOCl reaction with HCl, the physical uptake of HOCl in H₂SO₄ solution needs to be excluded when deducing γ 's based on the HOCl loss. As a result, some

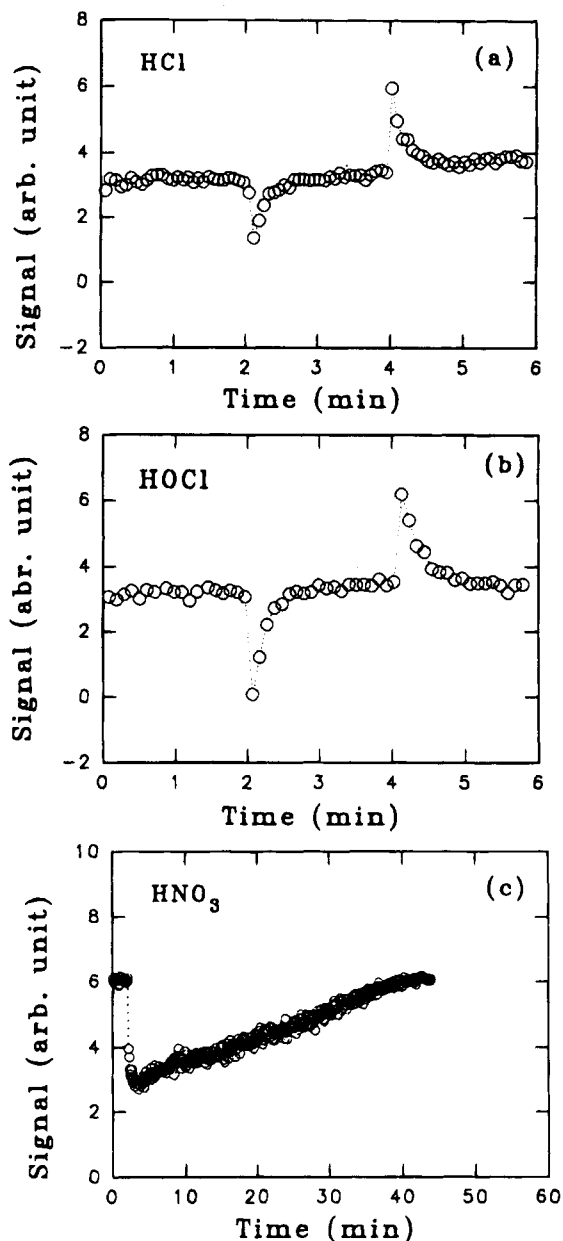


Figure 2. Physical uptake of HCl, HOCl, and HNO₃ when exposed to a 10-cm length of sulfuric acid film at $P_{\text{H}_2\text{O}} = 3.8 \times 10^{-4}$ Torr: (a) for HCl at 202 K and $P_{\text{HCl}} = 5 \times 10^{-7}$ Torr, (b) for HOCl at 204 K and $P_{\text{HOCl}} = 1 \times 10^{-7}$ Torr, and (c) for HNO₃ at 202 K and $P_{\text{HNO}_3} = 5 \times 10^{-7}$ Torr. The injector was moved upstream at 2 min and, for a and b, returned to its original position at 4 min. The average flow velocity of the carrier gas was 890 cm s⁻¹.

direct measurements of HCl, HOCl, and HNO₃ uptakes from the gas phase were carried out. These measurements also provide information on the time scale for reaching gas and liquid phase equilibrium.

To perform the uptake experiment, a steady-state flow of the adsorbed gas was first established through one of the injectors pushed in just downstream of the liquid sulfuric acid film (the jacked injector was only used for HNO₃). The injector was then quickly pulled upstream, exposing a section of the film to the vapor while monitoring its mass spectrometer signal. Examples of these results are shown in Figure 2 at a H₂O partial pressure of 3.8×10^{-4} Torr. In Figure 2a, a 10-cm length of sulfuric acid film was exposed to HCl at 2 min: the HCl concentration in the gas phase fell instantly upon pulling the injector and then returned to its original value as the film was saturated with HCl. At this point, no further uptake was

observed, suggesting that an equilibrium had been reached between the gas and liquid. At 4 min, the injector was pushed back, resulting in a similar, yet opposite, peak due to HCl desorption. Both the adsorption and desorption occurred on a time scale of less than 1 min. An HCl partial pressure of 5×10^{-7} Torr was used in this experiment. In sulfuric acid, HCl undergoes dissociation, dependent on the acidic content;³⁷ its reactive form is likely to be Cl^- .

Plotted in Figure 2b is the HOCl signal as it evolved with time due to exposure of a 10-cm length of sulfuric acid film at the HOCl partial pressure of 1×10^{-7} Torr. This uptake is qualitatively similar to that for HCl. Though a weak acid, HOCl also dissociates in highly acidic H_2SO_4 solutions.¹⁶ As can be concluded from Figure 2b, as long as sufficient time is allowed to saturate the acid film, reaction probabilities for the ClONO_2 hydrolysis (or HOCl reaction with HCl) can be accurately derived on the basis of the HOCl growth (or decay).

In contrast, HNO_3 uptake by the 10-cm H_2SO_4 film was substantial (Figure 2c); it took about 45 min to reach saturation for the HNO_3 partial pressure of 5×10^{-7} Torr. As shown in Figure 2c, the slow recovery in HNO_3 after the initial drop is most likely controlled by interfacial mass transport or by liquid phase diffusion. The significant uptake of HNO_3 by sulfuric acid is consistent with the formation of a $\text{H}_2\text{SO}_4/\text{HNO}_3/\text{H}_2\text{O}$ ternary system at this temperature, as noted in the Introduction section. The extent of HNO_3 dissociation in sulfuric acid is also dependent on acidity.³⁷

Both the absorption and desorption curves, as displayed in Figure 2, can be applied to extract information such as the product of the Henry's law solubility constant (H) and square root of the liquid diffusion coefficients ($D_l^{1/2}$). For example, the values in Figure 2 correspond to 25 and 41 (in the units of $\text{M atm}^{-1} \text{cm s}^{-1/2}$) for HCl and HOCl. Over the few measurements taken in this work, the results are generally in good agreement with those reported by Hanson and Ravishankara.³⁸

As expected, at a given H_2O partial pressure, we have observed drastic increases in the uptake with decreasing temperature, indicating very strong negative temperature dependencies. For conditions similar to those in Figure 2a, the time scale for HCl saturation (i.e., the time for the signal to return to its initial level) was as long as about 15 min at 195 K, whereas the HCl uptake was undetectable at 220 K. In general, solubilities of these species in H_2SO_4 increase with decreasing temperature at a given acid content and increase with decreasing H_2SO_4 content at a given temperature. Since the H_2O partial pressure was held constant in our experiments, temperature dependencies of these uptakes were actually 2-fold: at low temperatures the solubilities increased due to both decreasing temperature and decreasing H_2SO_4 content.

It should be pointed out that here we examine only the qualitative behavior of these uptake phenomena in terms of relevance to the present work. Detailed studies have been reported by Hanson and Ravishankara.³⁸

Reaction of ClONO_2 with H_2O . We have performed direct measurements of uptake coefficients for ClONO_2 on liquid sulfuric acid films at temperatures between 195 and 220 K and at a H_2O partial pressure of 3.8×10^{-4} Torr. Reaction probabilities (γ_1) were obtained by observing the decay of ClONO_2 or the growth of HOCl as a function of injector position as it was pulled successively upstream over the acid film.

A typical result of reactive uptake of ClONO_2 by sulfuric acid solution is shown in Figure 3 as time evolution of ClONO_2 and HOCl signals. The experiment was performed at 199 K and at a ClONO_2 partial pressure of 1×10^{-7} Torr. At ~ 2 min, a 10-cm length of H_2SO_4 film was exposed to ClONO_2

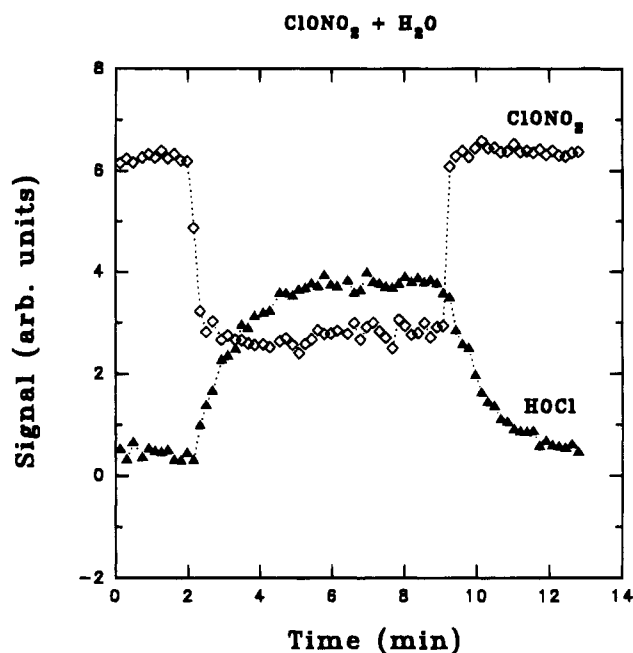


Figure 3. Temporal profiles of ClONO_2 and HOCl as ClONO_2 was exposed and not exposed to a 10-cm length of liquid sulfuric acid film. The HOCl signal exhibited a noticeable delay when the injector was positioned both upstream and downstream, as a result of HOCl being physically dissolved in sulfuric acid. Experimental conditions: $P_{\text{ClONO}_2} = 1 \times 10^{-7}$ Torr, $P_{\text{H}_2\text{O}} = 3.8 \times 10^{-4}$ Torr, $P_{\text{He}} = 0.5$ Torr, flow velocity = 897 cm s^{-1} , and $T = 199 \text{ K}$.

by pulling the injector upstream, and the signal of ClONO_2 dropped sharply to a very small value while the HOCl signal rose; at ~ 9.2 min, the injector was moved back downstream to stop the exposure and both the ClONO_2 and HOCl signals returned to their initial levels. The HOCl signal is found to exhibit a noticeable delay of about 1.5 min when the injector was positioned both upstream and downstream, consistent with the above-mentioned uptake behavior. As displayed in the figure, the product that leaves the surface is identified as HOCl; the other product, HNO_3 , is left behind on the film since it is very soluble in the cold sulfuric acid solutions.¹⁵ In all of our experiments of this type, the maximum signal due to HOCl was always comparable to the initial ClONO_2 signal. Because the relative detection sensitivity of the mass spectrometer for the two molecules was approximately the same, the measurements suggest that ClONO_2 reacting with H_2O on liquid sulfuric acid yields one HOCl.

In addition to the ClONO_2 reaction with H_2O , some loss of ClONO_2 may be related to its physical uptake by sulfuric acid. In our experiments, however, it is virtually impractical to separate the two processes. Nevertheless, this should have a negligible effect on the γ measurements, because we obtained essentially the same γ 's based on both ClONO_2 decay and HOCl growth, as discussed below. Hanson and Ravishankara²⁹ reported a solubility constant of about 10^3 M atm^{-1} for ClONO_2 in a 60% H_2SO_4 solution at 202 K.

Figure 4 is a semilog plot of measured ClONO_2 and HOCl signals versus injector position for an experiment performed at 199 K and at an initial ClONO_2 partial pressure of 1.2×10^{-7} Torr. The slope of the ClONO_2 decay line yields the first-order rate coefficient. The nearly constant concentration for HOCl at larger injector distance can be viewed as an asymptotic value. Hence, a plot of $\log(S_{\text{HOCl}}(\infty) - S_{\text{HOCl}}(z))$ versus injector distance (where z is the injector position and $S_{\text{HOCl}}(\infty)$ is the asymptotic HOCl signal at large injector distance, estimated visually from the figure) should be linear (Figure 4b). The slope of such a

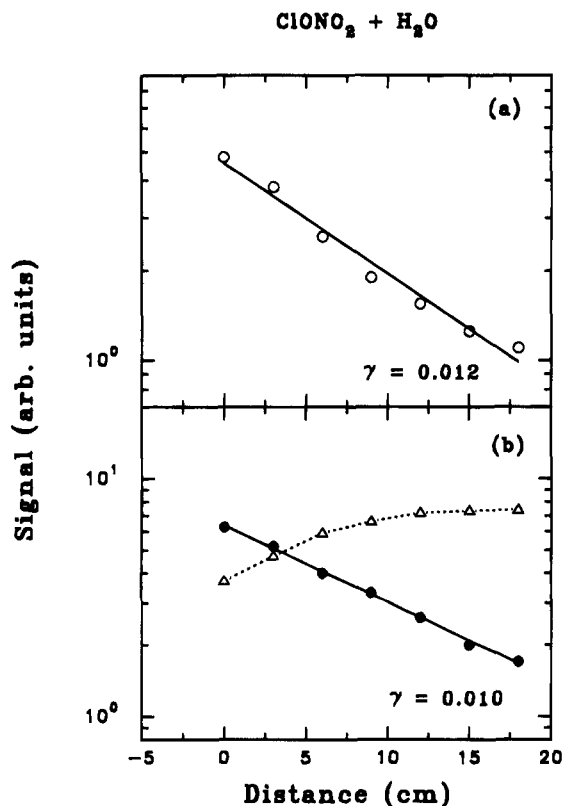


Figure 4. ClONO₂ and HOCl as a function of injector position, z : (a) \circ for ClONO₂ decay; (b) \triangle for HOCl growth; \bullet for plot of $S_{\text{HOCl}}(\infty) - S_{\text{HOCl}}(z)$ where $S_{\text{HOCl}}(\infty)$ is the HOCl signal at larger distance (see text for details). Both ClONO₂ decay and HOCl growth are found to follow first-order kinetics, yielding reaction probabilities of 0.012 and 0.010, respectively. Experimental conditions: $P_{\text{ClONO}_2} = 1.2 \times 10^{-7}$ Torr, $P_{\text{H}_2\text{O}} = 3.8 \times 10^{-4}$ Torr, $P_{\text{He}} = 0.5$ Torr, flow velocity = 921 cm s⁻¹, and $T = 199$ K.

plot also yields a first-order rate coefficient. Both the ClONO₂ decay and HOCl growth validate the first order kinetics. These coefficients lead to reaction probabilities of 0.012 and 0.010, corresponding to the ClONO₂ decay and HOCl growth, respectively. Note that the reaction probability obtained from the HOCl growth is very sensitive to the determination of the asymptotic value of $S_{\text{HOCl}}(\infty)$. For smaller reactive uptake of ClONO₂ (i.e., at high temperatures), a longer injector distance is needed to derive its value.

In Figure 5, values of γ_1 calculated from experiments such as those displayed in Figure 4 are presented as a function of temperature using $P_{\text{ClONO}_2} = 8 \times 10^{-8}$ to 2×10^{-7} Torr. The open circles denote γ_1 's obtained from the ClONO₂ decay, and the solid circles are based on the HOCl growth. The solid line is a polynomial fit through the data; the coefficients are summarized in Table 1 along with the experimental conditions. The estimated error limit of the γ_1 values is approximately $\pm 30\%$, which includes the uncertainties in measuring the first-order rate constant and in correcting for gas phase diffusion.

It is shown in the figure that, as the temperature varies from 220 to 196 K, γ_1 changes from about 3×10^{-4} to 0.03, increasing by 2 orders of magnitude. At the same time, the H₂SO₄ film is diluted from about 70 wt % to less than 50 wt %. Thus, the ClONO₂ hydrolysis shows a strong dependence on sulfuric acid content, in contrast to N₂O₅.²⁰⁻²³ Also, these measurements do not discriminate the effects of surface versus bulk reactions and represent only the overall process. For stratospheric applications, however, the measured γ 's need to be corrected for the finite dimension of the sulfate aerosols; this will be discussed in a later section.

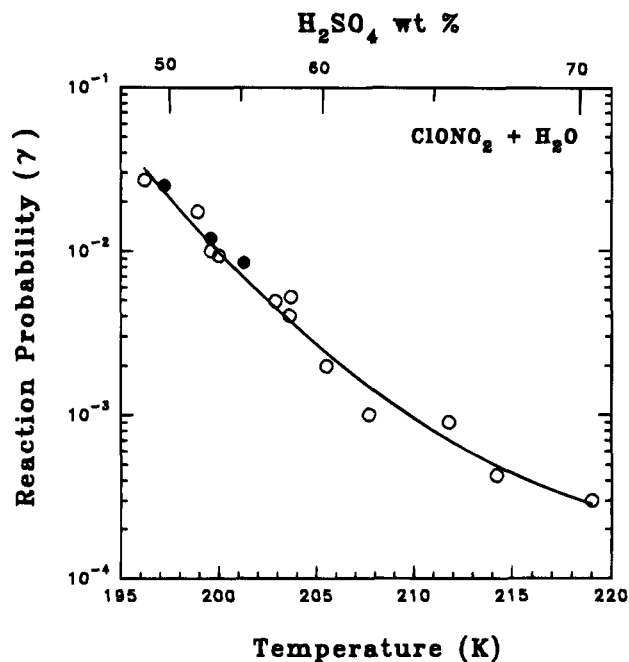


Figure 5. Reaction probability (γ_1) for ClONO₂ hydrolysis on liquid sulfuric acid films as a function of temperature at $P_{\text{H}_2\text{O}} = 3.8 \times 10^{-4}$ Torr. Open circles are γ_1 's determined from ClONO₂ decay, and solid ones from HOCl growth. The solid curve is a polynomial fit to the experimental data, and the coefficients are summarized in Table 1. The top axis corresponds to H₂SO₄ wt % estimated from the temperature and $P_{\text{H}_2\text{O}}$ based on vapor pressure data of sulfuric acid solutions.^{18,31} Experimental conditions: $P_{\text{ClONO}_2} = 8 \times 10^{-8}$ to 2×10^{-7} Torr, $P_{\text{He}} = 0.5$ Torr, and flow velocity = 890–925 cm s⁻¹.

Reaction of ClONO₂ with HCl. We investigated the reactive uptake of ClONO₂ by liquid H₂SO₄ in the presence of HCl vapor (γ_2): the measurements were performed by first allowing the substrate to equilibrate with HCl vapor introduced into the flow tube with He through one of the unjacketed injectors.

Figure 6 illustrates ClONO₂, HCl, HOCl, and Cl₂ signals as a function of the injector position with (a) $P_{\text{HCl}} > P_{\text{ClONO}_2}$ and (b) $P_{\text{ClONO}_2} > P_{\text{HCl}}$, conducted at 203 K. An important difference between parts a and b of Figure 6 is that with higher ClONO₂ partial pressures both Cl₂ and HOCl were liberated into the gas phase, whereas with HCl in excess no release of HOCl into the gas phase was observed. In Figure 6a, γ_2 can be calculated from the decay of the ClONO₂ signal or the growth of Cl₂ as a function of the ClONO₂ injector position, both yielding a reaction probability of about 0.02 (the difference is less than 10%). Correcting the measured ClONO₂ and Cl₂ signals for their relative sensitivities gave a yield of near unity for Cl₂. With $P_{\text{ClONO}_2} > P_{\text{HCl}}$ (Figure 6b), the HCl decay was initially very fast as Cl₂ rose rapidly. During the process, little HOCl was released. At larger injector distances, the HCl and Cl₂ signals approached zero and an asymptotic value, respectively. The HOCl signal, on the other hand, rose in accord with the ClONO₂ loss. Clearly, at smaller injector distances, the reaction of ClONO₂ with HCl was dominant. A reaction probability of 0.013 was derived from the initial HCl decay or Cl₂ growth, similar to that in Figure 6a. When the gaseous HCl concentration diminished at larger distances, the ClONO₂ hydrolysis became apparent, with a reaction probability of 0.0035 (obtained from ClONO₂ decay). This later value is nearly identical to that of ClONO₂ hydrolysis determined above. Hence, with ClONO₂ in excess, both reactions 2 and 3 were observed, with reaction probabilities equal to those measured

TABLE 1: Summary and Parametrization^a of the Reaction Probability (γ) Measurements

reaction	coefficients			experimental conditions
	a_1	a_2	a_3	
$\text{ClONO}_2 + \text{H}_2\text{O}$	114.3935	-1.0396	0.002 29	$P_{\text{H}_2\text{O}} = 3.8 \times 10^{-4}$ Torr $P_{\text{ClONO}_2} = 8 \times 10^{-8}$ to 2×10^{-7} Torr $T = 195\text{--}220$ K
$\text{ClONO}_2 + \text{HCl}$	75.0581	-0.6158	0.001 17	$P_{\text{H}_2\text{O}} = 3.8 \times 10^{-4}$ Torr $P_{\text{ClONO}_2} = 8 \times 10^{-8}$ to 2×10^{-7} Torr $P_{\text{HCl}} = 3 \times 10^{-7}$ to 4×10^{-7} Torr $T = 195\text{--}212$ K
$\text{HOCl} + \text{HCl}$	-42.5380	0.5238	-0.001 57	$P_{\text{H}_2\text{O}} = 3.8 \times 10^{-4}$ Torr $P_{\text{HOCl}} = 9 \times 10^{-8}$ to 1×10^{-7} Torr $P_{\text{HCl}} = 3 \times 10^{-7}$ to 4×10^{-7} Torr $T = 195\text{--}212$ K

$$^a \log \gamma = a_1 + a_2 T + a_3 T^2.$$

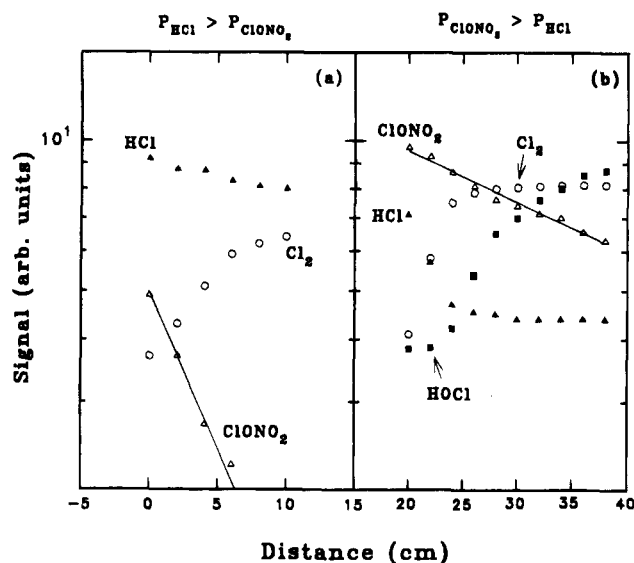


Figure 6. ClONO_2 (open triangles), HCl (solid triangles), Cl_2 (open circles), and HOCl (solid squares) as a function of injector position with (a) $P_{\text{HCl}} > P_{\text{ClONO}_2}$ (i.e., $P_{\text{ClONO}_2} = 1.4 \times 10^{-7}$ Torr and $P_{\text{HCl}} = 5.3 \times 10^{-7}$ Torr) and (b) $P_{\text{ClONO}_2} > P_{\text{HCl}}$ (i.e., $P_{\text{ClONO}_2} = 7.2 \times 10^{-7}$ Torr and $P_{\text{HCl}} = 3.3 \times 10^{-7}$ Torr). In a the reaction probabilities corresponding to ClONO_2 decay and Cl_2 growth are 0.022 and 0.020, respectively. In b the initial HCl decay at smaller injector distances leads to a reaction probability of 0.013, while the ClONO_2 decay at larger injector distances corresponds to a value of 0.0035. Experimental conditions: $P_{\text{H}_2\text{O}} = 3.8 \times 10^{-4}$ Torr, $P_{\text{He}} = 0.5$ Torr, flow velocity = 901 cm s^{-1} , and $T = 203$ K.

separately for the ClONO_2 hydrolysis and for the ClONO_2 reaction with HCl .

Some experiments were performed by varying the gaseous HCl concentration at a constant temperature. Figure 7 depicts the measured γ_2 's as a function of HCl partial pressure at 200 K and $P_{\text{ClONO}_2} \approx 8 \times 10^{-8}$ Torr (corresponding to a solution of about 54 wt %). It is evident that γ_2 varies with the HCl partial pressure: a change of P_{HCl} from 2×10^{-7} to 2×10^{-6} Torr results in γ_2 values from 0.02 to 0.19. This is primarily due to the increase in HCl dissolved in the film at higher HCl partial pressures, as governed by Henry's law (which linearly relates the concentration of gaseous HCl to that in the liquid).

Results of γ_2 measurements are shown in Figure 8 as a function of temperature. The open and filled symbols correspond to those determined from ClONO_2 decay and Cl_2 growth, respectively. The top axis labels H_2SO_4 wt % estimated from the H_2O vapor pressures in sulfuric acid solutions.^{18,31} In these experiments, the HCl partial pressures fluctuated only slightly in the range $(3\text{--}4) \times 10^{-7}$ Torr, and the initial partial pressures of HCl were always higher than those of ClONO_2 so that the pseudo first-order assumption applied ($P_{\text{ClONO}_2} = 8 \times$

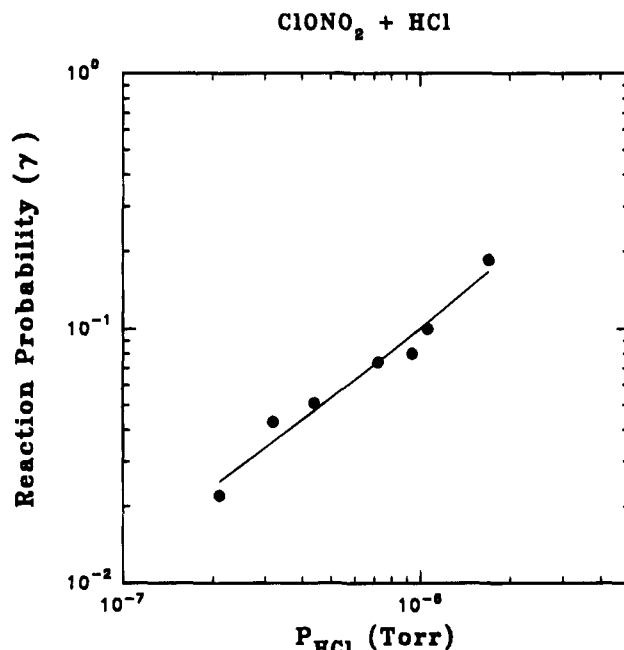


Figure 7. Reaction probabilities (γ_2) of ClONO_2 with HCl on liquid sulfuric acid films as a function of P_{HCl} . The solid curve is a polynomial fit to the experimental data. Experimental conditions: $P_{\text{ClONO}_2} \approx 8 \times 10^{-8}$ Torr, $P_{\text{H}_2\text{O}} = 3.8 \times 10^{-4}$ Torr, $P_{\text{He}} = 0.5$ Torr, flow velocity = $900\text{--}920 \text{ cm s}^{-1}$, and $T = 200$ K (corresponding to a solution of 54 wt %).

10^{-8} to 2×10^{-7} Torr). The parametrized temperature dependence of the γ_2 data is also listed in Table 1 with the experimental conditions. The uncertainty in the γ_2 values is approximately $\pm 30\%$ for $\gamma_2 < 0.1$. For larger γ_2 values (which are more sensitive to the gas phase diffusion), the uncertainty is as large as a factor of 4. Some scatter in γ_2 is also related to variation in HCl partial pressures during the various experiments; a P_{HCl} variation of $(3\text{--}4) \times 10^{-7}$ renders about a 20% difference in γ_2 , according to Figure 7.

In Figure 8, γ_2 approaches 0.3 at 195 K, whereas the value at 212 K is more than 2 orders of magnitude smaller. This profound temperature dependence appears to be correlated with the amount of dissolved HCl in the film: at a fixed $P_{\text{H}_2\text{O}}$ of 3.8×10^{-4} Torr, HCl solubility in H_2SO_4 increases by about 3 orders of magnitude over the temperature range from 210 to 195 K.^{37,38} As explained above, this solubility behavior is caused jointly by the changing temperature and changing H_2SO_4 content, when $P_{\text{H}_2\text{O}}$ is held constant.

At present the nature of this reaction mechanism is still unknown. On the ice surface it has been proposed that reaction 2 may occur in two steps, i.e., reaction 1 followed by reaction 3;^{39,40} it is also feasible that reaction 3 may enhance reaction 1

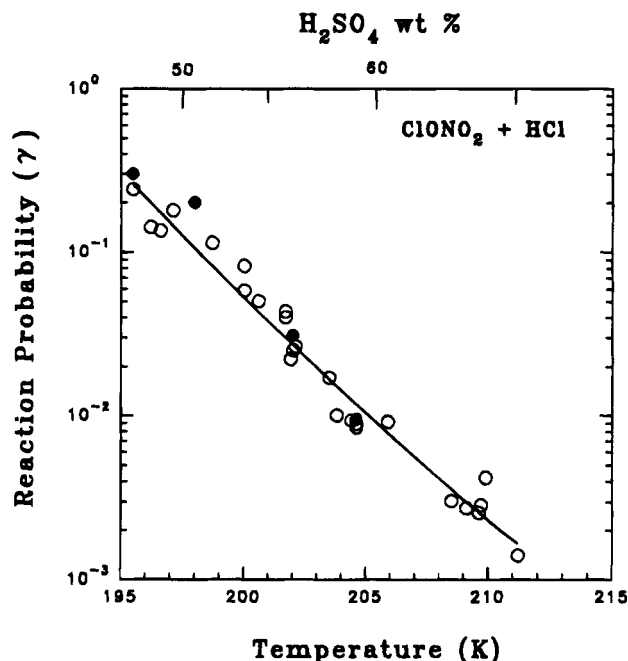


Figure 8. Reaction probability (γ_2) of ClONO₂ with HCl on liquid sulfuric acid films as a function of temperature at $P_{\text{H}_2\text{O}} = 3.8 \times 10^{-4}$ Torr. The open and filled symbols are γ_2 's determined from ClONO₂ decay and Cl₂ growth, respectively. The solid curve is a polynomial fit to the experimental data, and the coefficients are summarized in Table 1. Experimental conditions: $P_{\text{ClONO}_2} = 8 \times 10^{-8}$ to 2×10^{-7} Torr, $P_{\text{HCl}} = 3 \times 10^{-7}$ to 4×10^{-7} Torr, $P_{\text{He}} = 0.5$ Torr, and flow velocity = 890–925 cm s⁻¹.

by refreshing the liquid surface with H₂O. Alternatively, this reaction mechanism could simply be ClONO₂ reacting directly with HCl. As mentioned above, no appearance of HOCl was observed in the reaction of ClONO₂ with HCl, and almost all the ClONO₂ loss was accountable due to its reaction with HCl (which can be inferred from the Cl₂ rise). These observations do not enable us to separate the overall reaction into steps even if it were taking place in multiple steps. It is also likely that the measured ClONO₂ uptake in the presence of HCl is due to reactions with both HCl and H₂O. The relative importance of reactions 1 and 2 is discussed below.

Also, separation of the measured γ_2 as being due to reaction on the surface or in the bulk is not facile. Diffusion of ClONO₂ into the bulk and its subsequent reaction with dissolved HCl would enhance the uptake taking place at the surface. We did not observe any further changes in the ClONO₂ signal (nor Cl₂) after the initial decline (or rise) upon exposure of ClONO₂ to sulfuric acid, suggesting that either the bulk reaction was too small to compete with that on the surface or ClONO₂ diffusion was very rapid so that only the combined reaction was measured. Realization of these processes, however, could be important in calculating the reaction probabilities based on laboratory-measured first-order rate coefficients and solubility constants, as pointed out by Hanson and Ravishankara.²⁹

Reaction of HOCl with HCl. Reaction probability measurements between HOCl and HCl (γ_3) were conducted in the same manner as those for the ClONO₂ reaction with HCl. As stated previously, HOCl also physically dissolves in H₂SO₄ solutions. To better quantify the potential effect of HOCl dissolving in the film on the reaction probability, we determined γ_3 both from the HOCl decay and from the Cl₂ rise. Figure 9 shows signals due to HOCl, HCl, and Cl₂ versus injector position. Two different HOCl partial pressures were employed while the HCl partial pressure was held constant at 5×10^{-7} Torr. In Figure 9a, the observed first-order loss coefficient for HOCl gave a

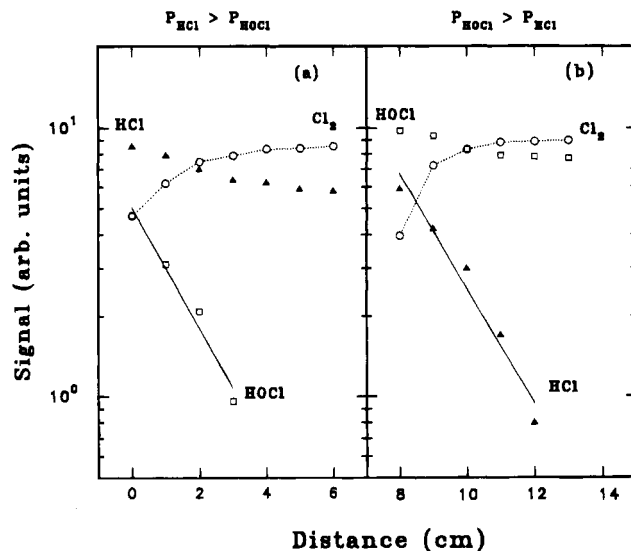


Figure 9. HOCl (open squares), Cl₂ (open circles), and HCl (solid triangles) as a function of injector position with (a) $P_{\text{HCl}} > P_{\text{HOCl}}$ ($P_{\text{HOCl}} = 9 \times 10^{-8}$ Torr) and (b) $P_{\text{HOCl}} > P_{\text{HCl}}$ ($P_{\text{HOCl}} = 7 \times 10^{-7}$ Torr). In a the reaction probabilities are 0.14 and 0.12, corresponding to HOCl decay and Cl₂ growth, while in b these values are 0.091 and 0.10. Experimental conditions: $P_{\text{HCl}} = 5 \times 10^{-7}$ Torr, $P_{\text{H}_2\text{O}} = 3.8 \times 10^{-4}$ Torr, $P_{\text{He}} = 0.5$ Torr, flow velocity = 901 cm s⁻¹, and $T = 198$ K.

reaction probability of 0.14 using $P_{\text{HOCl}} = 9 \times 10^{-8}$ Torr. The Cl₂ signal increased with injector distance in accord with the HOCl loss, with a corresponding value of 0.12. Over the length of the substrate, P_{HCl} decreased by about 30%. In Figure 9b, the HOCl partial pressure (7×10^{-7} Torr) slightly exceeded that of HCl. Again, both HOCl and HCl were lost as the Cl₂ signal increased. In this case, the decay of HCl followed the first-order rate law, with a γ_3 value of 0.091; the computed reaction probability based on the Cl₂ growth differed by about 15%. Also, since the amount of Cl₂ produced was comparable to the HOCl lost, we conclude that the decline in the HOCl signal is mainly due to the reaction with HCl. These observations also confirm the near unit stoichiometry for this reaction.

Results of γ_3 's measured at various HCl partial pressures are plotted in Figure 10. These experiments were performed at 202 K and $P_{\text{HOCl}} \approx 1 \times 10^{-7}$ Torr. The data in this figure display the expected behavior: γ_3 increases with increasing P_{HCl} . An increase in the reaction probability by a factor of 4 is observed as P_{HCl} is varied from 3×10^{-7} to 2×10^{-6} Torr. This is qualitatively the same as that for the ClONO₂ reaction with HCl described above.

The temperature dependence of the HOCl reaction with HCl is illustrated in Figure 11 using HOCl partial pressures of 9×10^{-8} to 1×10^{-7} Torr. The HCl partial pressure was maintained in the range $(3-4) \times 10^{-7}$ Torr. The symbols are the same as in Figure 8; coefficients of a polynomial fit of the data are summarized in Table 1. The estimated uncertainty for these measurements is similar to that discussed in the preceding section for the ClONO₂ reaction with HCl.

Reaction probabilities of HOCl with HCl are in general larger than those measured for ClONO₂ reacting with HCl (Figures 8 and 11) by a factor of 3–7. For example, γ_3 is greater than 0.3 at 197 K and decreases to about 0.004 at 215 K. This apparently reflects the higher solubility of HOCl in sulfuric acid: the Henry's law solubility coefficient for HOCl is about 1 order of magnitude greater than that for HCl under the same conditions.³⁸ The mechanism for the reaction of HOCl with HCl is likely to be acid-based catalysis, occurring after the uptake and subsequent solvation of both species,

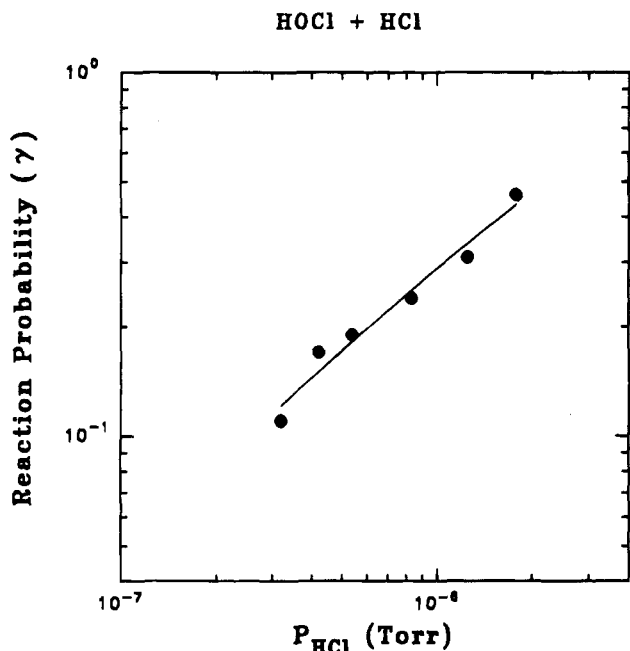


Figure 10. Reaction probabilities (γ_3) of HOCl with HCl on liquid sulfuric acid films as a function of P_{HCl} . The solid curve is a polynomial fit to the experimental data. Experimental conditions: $P_{\text{HOCl}} \approx 1 \times 10^{-7}$ Torr, $P_{\text{H}_2\text{O}} = 3.8 \times 10^{-4}$ Torr, $P_{\text{He}} = 0.5$ Torr, flow velocity = 890–925 cm s^{-1} , and $T = 202$ K.

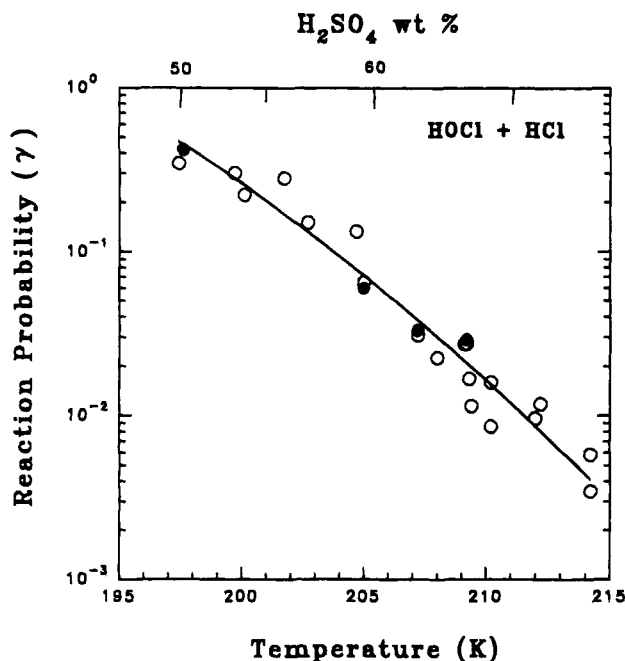
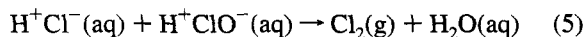


Figure 11. Reaction probability (γ_3) of HOCl with HCl on liquid sulfuric acid films as a function of temperature at $P_{\text{H}_2\text{O}} = 3.8 \times 10^{-4}$ Torr. The open and filled symbols are γ_3 's determined from the HOCl decay and Cl_2 growth, respectively. The solid curve is a polynomial fit to the experimental data, and the coefficients are summarized in Table 1. Experimental conditions: $P_{\text{HOCl}} = 9 \times 10^{-8}$ to 1×10^{-7} Torr, $P_{\text{HCl}} = 3 \times 10^{-7}$ to 4×10^{-7} Torr, $P_{\text{He}} = 0.5$ Torr, and flow velocity = 890–925 cm s^{-1} .



Reaction 5 has been investigated by Eigen and Kustin⁴¹ at room temperature. It was found to be limited by liquid phase diffusion.

The Effect of HNO_3 on Reactions 2 and 3. The effect of HNO_3 on reaction probabilities of HCl with ClONO_2 and HOCl

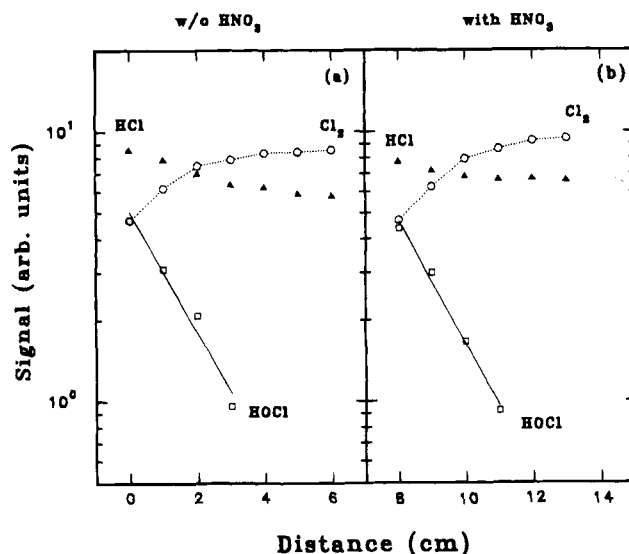


Figure 12. HOCl (open squares), Cl_2 (open circles), and HCl (solid triangles) as a function of injector position without (a) and with (b) HNO_3 . Both HOCl decay and Cl_2 growth with injector distance did not change appreciably with addition of HNO_3 . Figure 12a is the same as Figure 9a. In (b) the reaction probabilities are 0.135 and 0.140, corresponding to HOCl decay and Cl_2 growth. Experimental conditions: $P_{\text{HOCl}} = 1 \times 10^{-7}$ Torr, $P_{\text{HCl}} = 5 \times 10^{-7}$ Torr, $P_{\text{HNO}_3} = 5 \times 10^{-7}$ Torr, $P_{\text{H}_2\text{O}} = 3.8 \times 10^{-4}$ Torr, $P_{\text{He}} = 0.5$ Torr, flow velocity = 901 cm s^{-1} , and $T = 198$ K.

has been examined by first exposing the acid film to HCl and HNO_3 vapors and allowing them to equilibrate with the liquid. Because these experiments dealt virtually with the $\text{HNO}_3/\text{HCl}/\text{H}_2\text{SO}_4/\text{H}_2\text{O}$ quaternary system, it would be important to verify the reaction products or to look for possible new reactions, if any. Mass scans before and after exposure of ClONO_2 or HOCl to the quaternary solutions did not exhibit any new mass peaks over the entire mass range, indicating the reaction of ClONO_2 or HOCl with HCl to form Cl_2 in this multicomponent system. Also, there was no evidence for the occurrence of Cl_2O ($m/e = 86$), which has been suggested to form by the self-reaction of HOCl in sulfuric acid.²⁷

Figure 12 represents HOCl, HCl, and Cl_2 signals as a function of injector distance: both experiments were performed under the same conditions except that HNO_3 was present at a partial pressure of $\sim 5 \times 10^{-7}$ Torr in Figure 12b. As apparent in this figure, the HOCl decay (or Cl_2 growth) with injector distance did not change noticeably with the addition of HNO_3 ; the resulting reaction probabilities were within 10%. Note that, although temperature and H_2O partial pressure in parts a and b of Figure 12 were the same, the concentrations of H_2SO_4 in the films were different. This is a result of changing H_2SO_4 content in the $\text{H}_2\text{SO}_4/\text{HNO}_3/\text{H}_2\text{O}$ ternary system; at a given temperature, addition of HNO_3 to sulfuric acid solutions lowered the H_2O partial pressure so that extra H_2O was needed to hold the H_2O partial pressure constant. A similar phenomenon affects the sulfate aerosol composition in the stratosphere.^{15,16}

Results of reaction probabilities for reaction 3 performed on the $\text{H}_2\text{SO}_4/\text{HNO}_3/\text{HCl}/\text{H}_2\text{O}$ quaternary system are displayed in Figure 13 in the temperature range 198–209 K, along with the measured γ_3 's excluding HNO_3 (the same as the solid line in Figure 11). At 198 K, the liquid film could contain as much as 5 wt % HNO_3 , inferred from the ternary vapor pressure data of Zhang et al.¹⁵ Clearly, the difference in the reaction probabilities was negligible, considering experimental uncertainties and scatter in the present data.

Figure 14 shows ClONO_2 , HCl, and Cl_2 signals versus injector position for experiments (a) without and (b) with HNO_3 . A

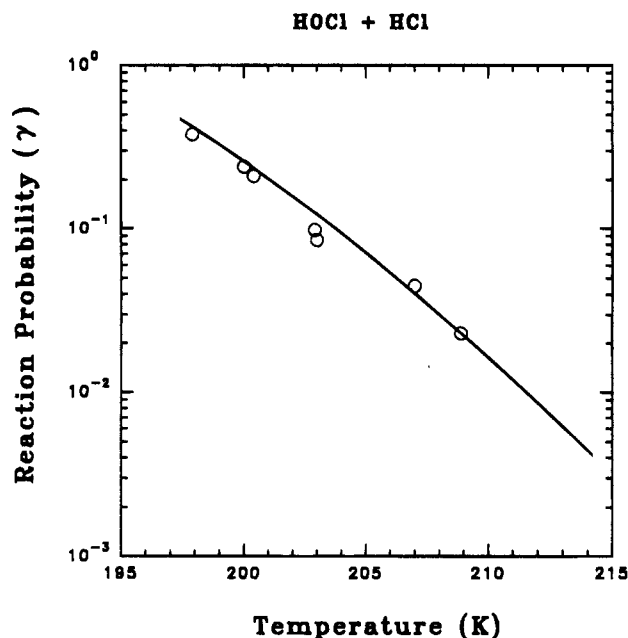


Figure 13. Reaction probability (γ_3) of HOCl with HCl on liquid sulfuric acid films doped with HNO₃, as a function of temperature at $P_{\text{H}_2\text{O}} = 3.8 \times 10^{-4}$ Torr. The solid curve is γ_3 determined earlier without HNO₃. Experimental conditions: $P_{\text{HOCl}} = 9 \times 10^{-8}$ to 1×10^{-7} Torr, $P_{\text{HCl}} = 3 \times 10^{-7}$ to 4×10^{-7} Torr, $P_{\text{He}} = 0.5$ Torr, $P_{\text{HNO}_3} = 5 \times 10^{-7}$ Torr, and flow velocity = 890–925 cm s⁻¹.

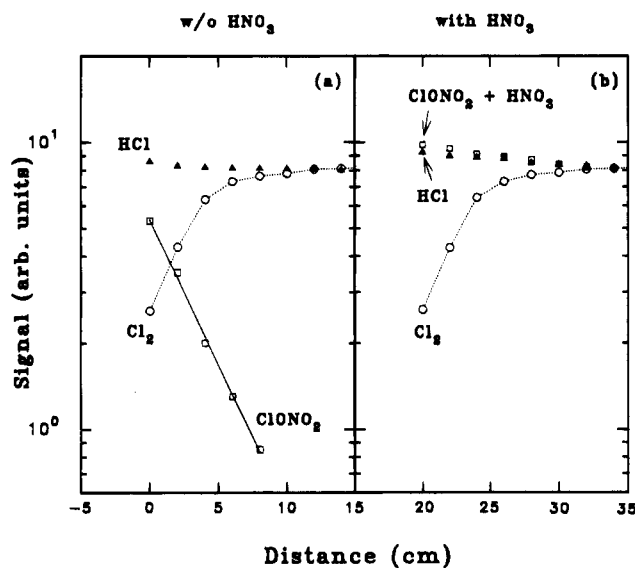


Figure 14. ClONO₂ (open squares), Cl₂ (open circles), and HCl (solid triangles) as a function of injector position without (a) and with (b) HNO₃. The Cl₂ growth with injector distance did not change appreciably with addition of HNO₃. In a the reaction probabilities are 0.042 and 0.045, corresponding to ClONO₂ decay and Cl₂ growth, while in b the value is 0.046 for Cl₂ growth. Experimental conditions: $P_{\text{ClONO}_2} = 1 \times 10^{-7}$ Torr, $P_{\text{HCl}} = 4 \times 10^{-7}$ Torr, $P_{\text{HNO}_3} = 5 \times 10^{-7}$ Torr, $P_{\text{H}_2\text{O}} = 3.8 \times 10^{-4}$ Torr, $P_{\text{He}} = 0.5$ Torr, flow velocity = 911 cm s⁻¹, and $T = 200$ K.

complication in Figure 14b is that ClONO₂ decay can no longer be employed to derive the first-order coefficient because of the interference from HNO₃. This problem, however, can be remedied by using the Cl₂ growth in both cases. Again, addition of HNO₃ did not appear to influence the Cl₂ growth as a function of the injector distance. Reaction probabilities derived from Figure 14a,b agreed within 10%.

The fact that reaction probabilities for reactions 2 and 3 are not significantly affected due to the incorporation of HNO₃ into

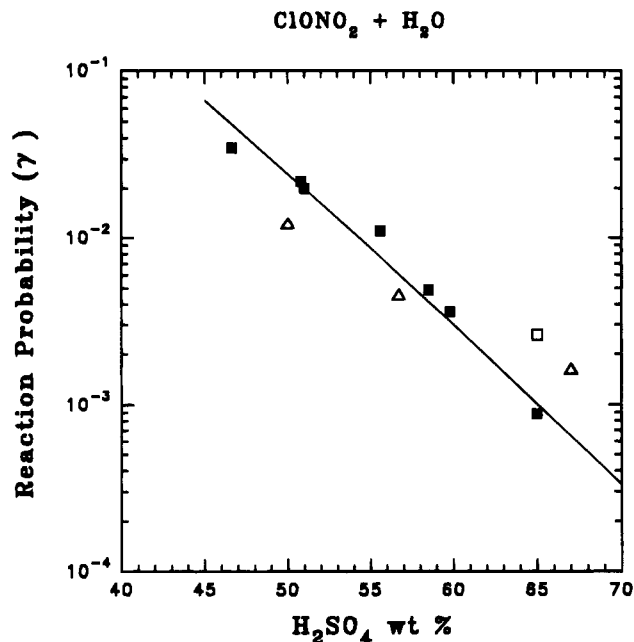


Figure 15. Comparison of reaction probabilities for ClONO₂ hydrolysis among various studies: Hanson and Ravishankara²⁹ (■), Williams et al.⁴¹ (Δ), and Tolbert et al.²⁷ (□). The solid line represents a fit of the present data.

H₂SO₄ solutions is intriguing. A possible explanation is that both reactions produce Cl₂, which does not dissolve in sulfuric acid. Furthermore, at a given H₂O partial pressure, the dissolution of HNO₃ in sulfuric acid does not significantly alter the HCl solubility at temperatures near 200 K; instead, it may make HCl slightly more soluble, by reducing the H₂SO₄ content.³⁷

Discussion

Comparison with Previous Results. The ClONO₂ hydrolysis on liquid sulfuric acid has been previously investigated by several groups.^{22,27,29,42} In Figure 15, comparison is made between the present results and previous measurements. The open square is data measured at 210 K by Tolbert et al.;²⁷ the open triangles are data at 223 K from Williams et al.⁴² Both studies used a Knudson cell technique. The solid squares are the most recent measurements from Hanson and Ravishankara²⁹ at 202 K. Shown as the solid line is the fit of the present data, converted to H₂SO₄ wt % on the basis of the temperature and H₂O partial pressure. The reaction probabilities we obtained are in good agreement with those reported by Hanson and Ravishankara, whereas our values are slightly higher (or lower) than those from the SRI group in less (or more) concentrated H₂SO₄ solutions.

Figure 16 compares our results of reaction 2 with the measurements of Hanson and Ravishankara.²⁹ They investigated γ_2 dependence on the HCl partial pressure at 202 K. The data from their measurements, plotted as the solid squares, are taken at $P_{\text{HCl}} \approx 4 \times 10^{-7}$ Torr. Note that the HCl solubility in sulfuric acid depends on both temperature and acid content, as discussed before. Therefore, the temperature difference at which the two measurements were carried out could result in a difference in the amounts of HCl in the solutions, even if the acid content was the same. Nevertheless, the agreement between the two studies is excellent. Theoretical predictions of uptake coefficients for reaction 2 by Hanson et al.,²⁸ however, yield results almost 1 order of magnitude smaller than those shown in Figure 16.

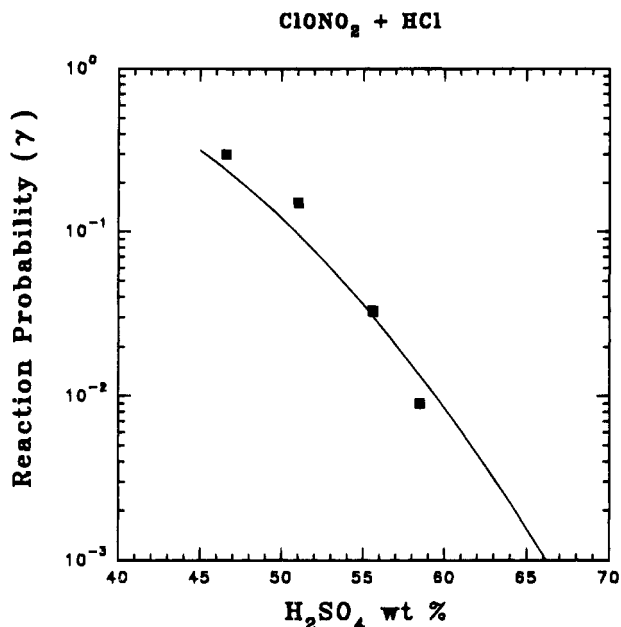


Figure 16. Comparison of reaction probabilities for ClONO₂ with HCl between this work (solid line) and those reported by Hanson and Ravishankara²⁹ (solid squares).

Available laboratory data of reaction probabilities for reaction 3 on sulfuric acid are rather limited. Hanson and Ravishankara^{22,38} studied this reaction for a 60 wt % H₂SO₄ solution: a value of $1.6 \times 10^5 \text{ M}^{-1} \text{ s}^{-1}$ for the second-order rate coefficient, k^{II} , was inferred. On the basis of our measured γ_3 's, we estimate this rate coefficient directly using⁴³

$$1/\gamma_3(\text{obs}) = 1/\alpha + \omega/[4H^*RT(D_1k^{\text{I}})^{1/2}] \quad (6)$$

where α is the mass accommodation (assumed unity here), R is the gas constant, T is the temperature, ω is the mean molecular speed, and $k^{\text{I}} = k^{\text{I}}[\text{HCl}]$ is the pseudo-first-order rate coefficient for the reaction of HOCl with HCl in the liquid. Values of liquid phase diffusion coefficients (D_1) and effective Henry's law coefficients (H^*), needed to extract k^{II} , are taken from the results of Hanson and Ravishankara.³⁸ The calculated k^{II} ranges from 1.35×10^5 to about $1.0 \times 10^4 \text{ M}^{-1} \text{ s}^{-1}$ for acid contents from 60 to 50 wt %: for the 60 wt % H₂SO₄, the value for k^{II} is consistent with that reported by Hanson and Ravishankara.^{22,38} The γ_3 's computed by Hanson et al.,²⁸ assuming a constant k^{II} , exhibit some systematic departure from the present results.

Relative Importance between ClONO₂ Hydrolysis and ClONO₂ Reaction with HCl. As discussed above, in the experiments when HCl is absent, HOCl is the only product of the reaction of ClONO₂ with H₂O. With addition of gaseous HCl at a partial pressure of $(3-4) \times 10^{-7}$ Torr (which is equivalent to the HCl mixing ratio of a few ppbv in the stratosphere), no HOCl is liberated into the gas phase when HCl is in excess over ClONO₂. These results may lead to the conclusion that ClONO₂ hydrolysis will be less important because no gaseous HOCl can be produced. This, however, may not be necessarily true for submicron-sized sulfate aerosols in the stratosphere. Consider a spherical droplet of radius a . The characteristic time for liquid diffusion within the particle is given by⁴⁴

$$t = a^2/(\pi^2 D_1) \quad (7)$$

This diffusion time needs to be compared with the reaction time of HOCl with dissolved HCl (given by the inverse of the first

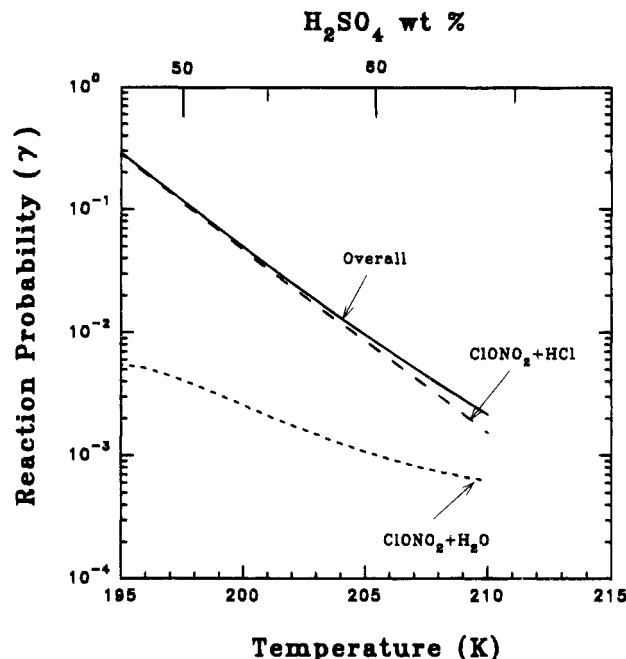


Figure 17. Partitioning of the overall uptake coefficients of ClONO₂ with dissolved HCl (solid curve) into those due to ClONO₂ hydrolysis (short-dashed curve) and due to ClONO₂ reaction with HCl (long-dashed curve), using eqs 8–10. See text for details.

order loss rate coefficient, $1/k^{\text{I}}$) to determine the overall reaction product on the droplet. For a stratospheric aerosol of about $0.1 \mu\text{m}$, the ratio of diffusion to reaction time constants is on the order of 10^{-3} – 10^{-2} . Therefore, HOCl generated by the ClONO₂ hydrolysis will likely diffuse out of the droplet before having a chance to react with HCl.

In the case of two reactions (i.e. 1 and 2) competing in the liquid, as is the case in our measurements, the overall uptake coefficient shown in Figure 10 may be expressed as²⁸

$$1/\gamma_2(\text{obs}) = 1/\alpha + \omega/[4H^*RTD_1^{1/2}(k_{\text{H}_2\text{O}}^{\text{I}} + k_{\text{HCl}}^{\text{I}})^{1/2}] = 1/[\gamma_1(\text{obs})(1+r)^{1/2}] \quad (8)$$

where r is the ratio of the first-order loss rate coefficients for ClONO₂ reaction with H₂O ($k_{\text{H}_2\text{O}}^{\text{I}}$) and dissolved HCl ($k_{\text{HCl}}^{\text{I}}$). From 195 to 210 K, this ratio varies from 52 to 2.4, derived directly from our measured reaction probabilities of $\gamma_1(\text{obs})$ (Figure 5) and $\gamma_2(\text{obs})$ (Figure 8). These values of r are then used to calculate the fraction of ClONO₂ uptake due to reaction with HCl,

$$\gamma_2^{\text{HCl}} = r\gamma_2(\text{obs})/(1+r) \quad (9)$$

and due to reaction with H₂O

$$\gamma_2^{\text{H}_2\text{O}} = \gamma_2(\text{obs})/(1+r) \quad (10)$$

The results are portrayed in Figure 17: the calculated contribution of ClONO₂ hydrolysis to the overall uptake coefficient at temperatures of 200 and 210 K is about 6 and 30%, respectively. Clearly, at lower temperatures and at $P_{\text{HCl}} = (3-4) \times 10^{-7}$ Torr the reaction of ClONO₂ with dissolved HCl is dominant.

Correction for Finite Aerosol Sizes. Since reaction probabilities were measured on bulk liquid H₂SO₄ surfaces in this work, application of the present data to the stratosphere requires correction for the finite dimension of the sulfate aerosols. In general, the reaction probability on small aerosols (γ_c) is related to the laboratory measured (γ_m) value by^{28,44}

$$1/\gamma_c \approx 1/\alpha + 1/[\gamma_m(\coth q - 1/q)] \quad (11)$$

where q is the diffuso-reactive parameter, defined by $q = a(k^l/D_1)^{1/2}$ or $q = all$ (l is the diffuso-reactive length). We have used the diffuso-reactive length for ClONO₂ in sulfuric acid suggested by Hanson and Ravishankara,²⁹ which is inversely proportional to the square root of water activity. To estimate l for HOCl in sulfuric acid, we calculate the first-order loss coefficient based on the measured reaction probabilities of HOCl with HCl, using eq 6 and $H^*(D_1)^{1/2}$ measured by Hanson and Ravishankara.³⁸

Shown in Figure 18 are the reaction probabilities relevant to a nominal 0.1- μ m aerosol particle. Figure 18 indicates that γ_c is much smaller than γ_m for reaction 3, while γ_c is very close to γ_m for reactions 1 and 2. Note that the correction for the aerosol size is dependent on a knowledge of ClONO₂ solubility in sulfuric acid, which is not directly measurable. Also, available information on liquid phase diffusion coefficients in sulfuric acid is very limited. Hence, the treatment using eq 11 may introduce considerable uncertainty.

Reaction Probabilities on the H₂SO₄/HNO₃/H₂O Ternary System. We have shown in this work that uptake coefficients for reactions 2 and 3 do not change appreciably on the H₂SO₄/HNO₃/H₂O ternary solution compared to those on the H₂SO₄/H₂O binary solution at temperatures near or slightly less than 200 K. These measurements, however, are restricted to temperatures above 195 K, because of the freezing of the liquid film. In the stratosphere the composition of sulfate aerosols changes rapidly with decreasing temperature, by absorbing H₂O and HNO₃: at very low temperatures (<192 K) the aerosols could transform essentially into HNO₃ and H₂O binary solutions,^{13,15,16} if crystallization is inhibited. In light of previous laboratory observations that incorporation of HNO₃ in sulfuric acid may increase HCl solubility by reducing the H₂SO₄ content,³⁷ reactions 2 and 3 could be enhanced due to dissolution of HNO₃. The present results reveal that at temperatures near 195 K these reaction probabilities are already quite high, approaching a few tenths. As a result, it is likely that in very cold stratospheric regions the rate-limiting step is gas phase diffusion.

Conclusions

In this work we have investigated heterogeneous reactions 1–3 on liquid sulfuric acid surfaces. Reaction probabilities for these reactions have been measured in the temperature range 195–220 K: by maintaining a constant H₂O partial pressure typical of the lower stratosphere, we are able to simulate the composition representative of stratospheric sulfate aerosols. The data reveal that these reactions depend on temperatures or H₂SO₄ wt %. The reaction probability for ClONO₂ hydrolysis approaches 0.01 at temperatures below 200 K, whereas the values for ClONO₂ and HOCl reacting with HCl are on the order of a few tenths at 200 K. The results corroborate earlier findings that heterogeneous reactions involving ClONO₂, HCl, and HOCl could provide important pathways for chlorine activation at high latitudes in winter and early spring.^{13,28}

The relative importance or competition between ClONO₂ hydrolysis (reaction 1) and ClONO₂ reaction with HCl (reaction 2) has also been examined. The data imply that in the presence of gaseous HCl molecules at stratospheric concentrations the reaction of ClONO₂ with HCl is dominant at low temperatures (<200 K), but the ClONO₂ hydrolysis becomes important at temperatures above 210 K.

Lastly, at temperatures near 200 K or slightly less than 200 K, reaction probability measurements performed on the H₂SO₄/

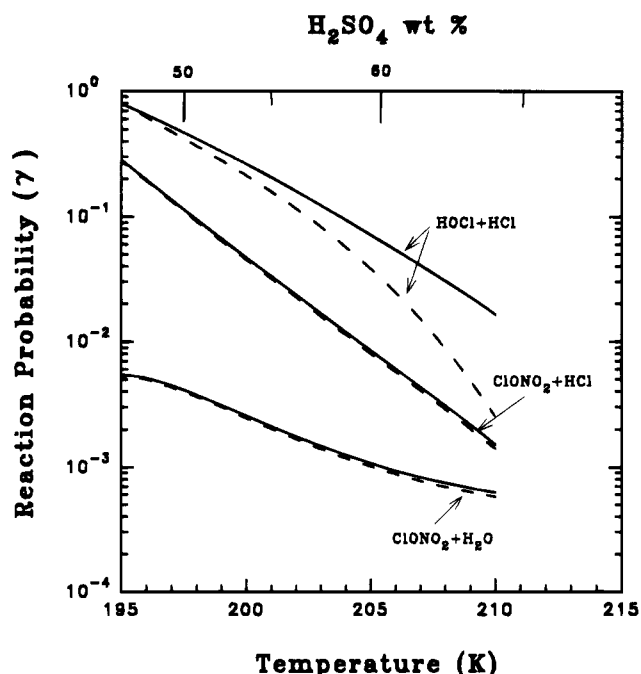


Figure 18. Corrected reaction probabilities (dashed curves) relevant to a nominal 0.1- μ m aerosol particle based on eq 11, along with those pertinent to the bulk solutions (solid curves). See text for details.

HNO₃/H₂O ternary solutions do not exhibit noticeable deviation from those performed on the H₂SO₄/H₂O binary system, showing little effect of HNO₃ in sulfate aerosols on the ClONO₂ and HOCl reactions with HCl. Our results suggest that at low temperatures (<195 K) these reaction probabilities are so large that gas phase diffusion is likely the rate-limiting step in the stratosphere.

Acknowledgment. We thank D. R. Hanson, M. J. Molina, A. Tabazadeh, and D. R. Worsnop for helpful discussions. The research described in this paper was performed at the Jet Propulsion Laboratory, California Institute of Technology, under a contract with the National Aeronautics and Space Administration.

References and Notes

- (1) Solomon, S. *Rev. Geophys.* **1988**, *26*, 131.
- (2) Anderson, J. G.; Brune, W. H.; Lloyd, S. A.; Starr, W. L.; Loewenstein, M.; Podolske, J. R. *J. Geophys. Res.* **1989**, *94*, 11480.
- (3) Anderson, J. G.; Toohey, D. W.; Brune, W. H. *Science* **1991**, *251*, 39.
- (4) Brune, W. H.; Anderson, J. G.; Toohey, D. W.; Fahey, D. W.; Kawa, S. R.; Jones, R. L.; McKenna, D. S.; Poole, L. R. *Science* **1991**, *252*, 1260.
- (5) Webster, C. R.; May, R. D.; Toohey, D. W.; Avallone, L. M.; Anderson, J. G.; Newman, P.; Lait, L.; Schoeberl, M. R.; Elkins, J. W.; Chan, K. R. *Science* **1993**, *261*, 1130.
- (6) DeMore, W. B.; Sander, S. P.; Golden, D. M.; Molina, M. J.; Hampson, R. F.; Kurylo, M. J.; Howard, C. J.; Ravishankara, A. R. *Chemical kinetics and photochemical data for use in stratospheric modeling*; JPL Publ. 92–20, NASA, 1992.
- (7) Toon, O. B.; Hamill, P.; Turco, R. P.; Pinto, J. *Geophys. Res. Lett.* **1986**, *13*, 1284.
- (8) Crutzen, P. J.; Arnold, F. *Nature* **1986**, *324*, 651.
- (9) Hofmann, D. J.; Solomon, S. *J. Geophys. Res.* **1989**, *94*, 5029.
- (10) Brasseur, G. P.; Granier, C.; Walters, S. *Nature* **1990**, *348*, 626.
- (11) Rodriguez, J. M.; Ko, M. K. W.; Sze, N. D. *Nature* **1991**, *352*, 134.
- (12) Steele, H. M.; Hamill, P.; McCormick, M. P.; Swissler, T. J. *J. Atmos. Sci.* **1983**, *40*, 2055.
- (13) Molina, M. J.; Zhang, R.; Wooldridge, P. J.; McMahon, J. R.; Kim, J. E.; Chang, H. Y.; Beyer, K. D. *Science* **1993**, *261*, 1418.
- (14) Toon, O.; Browell, E.; Gary, B.; Bait, L.; Newman, P.; Pueschel, R.; Russell, P.; Schoeberl, M.; Toon, G.; Traub, W.; Valero, F.; Selkirk, H.; Jordan, J. *Science* **1993**, *261*, 1136.

- (15) Zhang, R.; Wooldridge, P. J.; Molina, M. J. *J. Phys. Chem.* **1993**, *97*, 8541.
- (16) Tabazadeh, A.; Turco, R. P.; Jacobson, M. Z. *J. Geophys. Res.* **1994**, *99*, 12897.
- (17) Middlebrook, A. M.; Iraci, L. T.; McNeill, L. S.; Koehler, B. G.; Wilson, M. A.; Saastad, O. W.; Tolbert, M. A.; Hanson, D. R. *J. Geophys. Res.* **1993**, *98*, 20,473.
- (18) Zhang, R.; Wooldridge, P. J.; Abbatt, J. P. D.; Molina, M. J. *J. Phys. Chem.* **1993**, *97*, 7351.
- (19) Zhang, R.; Leu, M. T.; Keyser, L. F. Unpublished results.
- (20) Mozurkewich, M.; Calvert, J. G. *J. Geophys. Res.* **1988**, *93*, 15889.
- (21) Van Doren, J. M.; Watson, L. R.; Davidovits, P.; Worsnop, D. R.; Zahniser, M. S.; Kolb, C. E. *J. Phys. Chem.* **1991**, *95*, 1684.
- (22) Hanson, D. R.; Ravishankara, A. R. *J. Geophys. Res.* **1991**, *96*, 5081.
- (23) Fried, A.; Calvert, J. G.; Mozurkewich, M. *J. Geophys. Res.* **1994**, *99*, 3517.
- (24) Hanson, D. R.; Ravishankara, A. R. *J. Geophys. Res.* **1993**, *98*, 22931.
- (25) Zhang, R.; Jayne, J. T.; Molina, M. J. *J. Phys. Chem.* **1994**, *98*, 867.
- (26) Watson, L. R.; Van Doren, J. M.; Davidovits, P.; Worsnop, D. R.; Zahniser, M. S.; Kolb, C. E. *J. Geophys. Res.* **1990**, *95*, 5631.
- (27) Tolbert, M. A.; Rossi, M. J.; Golden, D. M. *Geophys. Res. Lett.* **1988**, *15*, 847.
- (28) Hanson, D. R.; Ravishankara, A. R.; Solomon, S. *J. Geophys. Res.* **1994**, *99*, 3615.
- (29) Hanson, D. R.; Ravishankara, A. R. *J. Phys. Chem.* **1994**, *98*, 5728.
- (30) Chu, L. T.; Leu, M. T.; Keyser, L. F. *J. Phys. Chem.* **1993**, *97*, 7779. *Ibid.* **1993**, *97*, 12798.
- (31) Zeleznik, F. J. *J. Phys. Chem. Ref. Data* **1991**, *20*, 1157.
- (32) Howard, C. J. *J. Phys. Chem.* **1979**, *83*, 3.
- (33) Brown, R. L. *J. Res. Natl. Bur. Stand. (U. S.)* **1978**, *83*, 1.
- (34) Marrero, T. R.; Mason, E. A. *J. Phys. Chem. Ref. Data* **1972**, *1*, 3.
- (35) Leu, M. T. *Geophys. Res. Lett.* **1988**, *15*, 17.
- (36) Jansco, G.; Puzezin, J.; Van Hook, W. A. *J. Phys. Chem.* **1970**, *74*, 2984.
- (37) Zhang, R. Ph.D. Dissertation, MIT, 1993.
- (38) Hanson, D. R.; Ravishankara, A. R. *J. Phys. Chem.* **1993**, *97*, 12309.
- (39) Abbatt, J. P. D.; Beyer, K. D.; Fucaloro, A. F.; McMahon, J. R.; Wooldridge, P. J.; Zhang, R.; Molina, M. J. *J. Geophys. Res.* **1992**, *97*, 15819.
- (40) Abbatt, J. P. D.; Molina, M. J. *J. Phys. Chem.* **1992**, *96*, 7674.
- (41) Eigen, M.; Kustin, K. *J. Am. Chem. Soc.* **1962**, *84*, 1355.
- (42) Williams, L. R.; Manion, J. A.; Golden, D. M. *J. Appl. Meteor.* **1994**, *33*, 785.
- (43) Worsnop, D. R.; Zahniser, M. S.; Kolb, C. E.; Gardner, J. A.; Watson, L. R.; Van Doren, J. M.; Davidovits, P. *J. Phys. Chem.* **1989**, *93*, 1159.
- (44) Schwartz, S. E. In *Chemistry of Multiphase Atmospheric Systems*; Jaeschke, W., Ed.; NATO ASI Series; NATO: Brussels, 1986; Vol. G6. JP942262R